

Reinforcement of osteogenic and mechanical properties of calcium phosphate cement with palm tocotrienol

Siti Sarah Md Dali¹, Ahmad Saqif Nazib¹, Nik Adlina Sofea Abd Rahim¹, Siti Nur Khadijah Sha'ari¹, Xin Qi Goh¹, Kok-Yong Chin¹, Fairus Ahmad², Sok Kuan Wong^{1*}

¹Department of Pharmacology, Faculty of Medicine, Universiti Kebangsaan Malaysia, Jalan Yaacob Latif, Bandar Tun Razak, Cheras, Kuala Lumpur, Malaysia

²Department of Anatomy, Faculty of Medicine, Universiti Kebangsaan Malaysia, Jalan Yaacob Latif, Bandar Tun Razak, Cheras, Kuala Lumpur, Malaysia

Submitted: 13 January 2025; Accepted: 6 April 2025

Online publication: 21 May 2025

Arch Med Sci

DOI: <https://doi.org/10.5114/aoms/203758>

Copyright © 2025 Termedia & Banach

*Corresponding author:

Sok Kuan Wong
Department of
Pharmacology
Faculty of Medicine
Universiti Kebangsaan
Malaysia
Jalan Yaacob Latif
Bandar Tun Razak
56000 Cheras
Kuala Lumpur, Malaysia
Phone: +603-9145 9566
E-mail: sokkuan@ukm.edu.my

Abstract

Introduction: Calcium phosphate cement (CPC) is a promising bone substitute but lacks osteogenicity and mechanical strength. This study investigated the effects of CPC doped with palm tocotrienol, a bone-protective agent, on bone regeneration in ovariectomised rats with tibial defects.

Material and methods: Female Sprague-Dawley rats were divided into sham-operated controls, ovariectomised rats (OVX), ovariectomised rats with bone defects implanted with CPC (OVX + CPC) and ovariectomised rats with bone defects implanted with palm tocotrienol-doped CPC (OVX + CPC/T3). A tibial bone defect was created 11 weeks after ovariectomy.

Results: Whole-body BMC was higher in OVX + CPC (10.89 ± 0.07 g) and OVX + CPC/T3 (11.26 ± 0.07 g) than OVX (10.24 ± 0.14 g) ($p < 0.05$). Whole-body BMD of OVX + CPC/T3 (0.175 ± 0.003 to 0.182 ± 0.003 g/cm³), left tibia BMC of OVX + CPC (0.308 ± 0.016 to 0.343 ± 0.022 g) and OVX + CPC/T3 (0.313 ± 0.020 to 0.343 ± 0.016 g) increased from week 11 to 15 ($p < 0.05$). The OVX + CPC/T3 group had higher bone stiffness (23.31 ± 1.07 vs. 8.35 ± 3.84 N/mm), collagen (scoring: 3 ± 0.75 vs. 2 ± 0), trabecular bone formation (scoring: 3 ± 0 vs. 2 ± 0), and trabecular bone volume (36.30 ± 3.58 vs. 20.86 ± 1.03%) but lower osteoclast surface (1.65 ± 0.49 vs. 6.60 ± 1.36%) than OVX ($p < 0.05$). Tibial BMP-2 in OVX + CPC/T3 (78.96 ± 8.30 pg/mg protein) was higher than OVX (30.65 ± 3.69 pg/mg protein) and OVX + CPC (48.09.96 ± 8.39 pg/mg protein) ($p < 0.05$). Tibial Runx-2 in OVX + CPC/T3 (2589.75 ± 204.74 pg/mg protein) was higher than OVX (1652.97 ± 156.85 pg/mg protein) and OVX + CPC (1845.77 ± 158.17 pg/mg protein) ($p < 0.05$).

Conclusions: Palm tocotrienol enhanced the osteogenic properties of CPC, promoting collagen and trabecular bone formation in ovariectomised rats with bone defects. These findings suggest its potential to overcome the drawbacks of CPC and promote bone regeneration.

Key words: bone regeneration, bone substitutes, osteoporosis, vitamin E.

Introduction

The physiological process of bone remodelling involves the removal of old or damaged bone by osteoclasts (the bone-resorbing cells) and the formation of new bone by osteoblasts (the bone-forming cells). The process involves the careful regulation and maintenance of a balance between osteoclast-mediated bone resorption and osteoblast-mediated bone for-

mation, ensuring no net changes in bone mass or mechanical strength in healthy individuals [1]. A bone defect is the loss of bone tissue resulting from surgery (resection of tumour), congenital malformation, diseases (osteoporosis and osteosarcoma), high-energy trauma (fractures), and infections (osteomyelitis) [2]. Bone remodelling represents the last stage of natural self-repair mechanisms after haematoma formation, inflammation, tissue granulation, and callus creation [3, 4]. Osteoporosis is a systemic skeletal disease characterised by low bone mass and microstructural deterioration caused by a disruption in bone remodelling whereby bone resorption exceeds bone formation [5]. Animal studies have demonstrated that compromised bone metabolism negatively affects the repair process by slowing cellular differentiation, reducing callus formation and impairing bone mineralisation [6, 7]. In addition, clinical studies have identified poor bone quality as a risk factor for non-union fracture and delayed healing [8–10].

Bone graft offers a regenerative solution by supplying tissue to the defect, fostering integration, promoting vascularisation, and facilitating local bone repair. Biomaterials from both natural and synthetic origins have been predominantly used to rectify bone defects. Autologous bone grafts are the gold standard due to their osteoconductive, osteoinductive, and osteogenic properties, along with a low risk of infectious and immunologic complications [11]. The major disadvantages of autologous bone grafting include donor site injury, morbidity, deformity, higher costs, and high surgical risks, such as bleeding, inflammation, infection and chronic pain [12]. The use of allogeneic and xenogeneic bone grafts is limited because of possible immunological rejection, pathogen transmission, as well as a lack of adequate integration and vascularisation with the host [13]. Thus, the development of bioactive materials that enhance skeletal regeneration is crucial, particularly for conditions associated with low bone mass. Artificial bone graft is favourable for its unlimited supply, low risk of disease transmission or immunoreaction, ease of sterilisation and storage, adaptability in various shapes and sizes for surgery, scar reduction and minimally invasive procedure [14].

Calcium phosphate cement (CPC) is a biomaterial composed of calcium phosphate powders and a liquid phase capable of self-setting *in situ*, forming a supportive scaffold [15]. It chemically resembles natural bone, thus serving as a promising hard tissue substitute to repair bone defects. Their advantageous properties include good biocompatibility, bioactivity, osteoconductivity, injectability, mouldability, resorbability, self-setting ability and feasibility in controlled drug delivery. However, the clinical appli-

cation of CPC as bone replacement is critically limited by its intrinsic poor mechanical properties and osteogenic capacity, necessitating functionalisation with bioactive compounds to enhance its therapeutic efficacy, particularly in osteoporotic conditions. Recent research attempted to address the limitations of CPC by incorporating it with biological (such as proteins, polysaccharides, or blood components) [2] and synthetic (such as polymers, biomimetics, or chemical elements) materials [16].

Tocotrienol and tocopherol are two different forms of vitamin E made up of four distinct analogues, namely alpha (α), beta (β), gamma (γ) and delta (δ)-isomers. They share a similar chromanol head but differ in the side chain structures. Tocotrienol has an unsaturated farnesyl tail, while tocopherol has a saturated phytyl tail. Compared to tocopherol, tocotrienol exhibited superior anti-inflammatory, antioxidative, cholesterol-lowering, and osteogenic properties [17]. Furthermore, tocotrienol demonstrated enhanced bioavailability [18] and higher cellular uptake [19] than tocopherol, suggesting more potent physiological activity of tocotrienol. Major dietary sources of tocotrienol include rice bran oil, annatto seeds, and palm fruits. The bone-protective property of tocotrienol has been extensively reviewed [20, 21]. Previous studies using animal models of osteoporosis induced by sex hormone deficiency [22], glucocorticoids [23], nicotine [24], and metabolic syndrome [25, 26] have demonstrated that oral supplementation of tocotrienol prevented bone loss. In addition, tocotrienol administration has been found to promote fracture healing in a rat model of postmenopausal osteoporosis [27, 28]. Tocotrienol modulated key regulators of bone metabolism, including inflammatory mediators, oxidative stress markers, growth factors, hormones, phosphate metabolism, and receptor activator of nuclear factor kappa-B ligand (RANKL)/osteoprotegerin (OPG) ratio [29, 30]. Given its osteogenic and bone healing potential, incorporating tocotrienol into CPC presents a novel strategy to enhance its regenerative capabilities. The effects of tocotrienol in enhancing the characteristics of CPC for bone regeneration in animals with oestrogen deficiency and bone defects remain unexplored.

This study aims to investigate the effects of CPC doped with palm tocotrienol on bone regeneration using an ovariectomised rat model tibial bone defect. We hypothesise that tocotrienol can improve the drawbacks of CPC by enhancing bone biomechanical strength and encouraging new bone formation at the defect site.

Material and methods

Treatment preparation

All the ingredients in powder form – including monocalcium phosphate monohydrate (MCPM)

(Sigma Aldrich, Germany), beta-tricalcium phosphate (β -TCP) (Sigma Aldrich, Germany), citric acid (Sigma Aldrich, Germany), and sodium hyaluronate (BBI Life Sciences, China) – were sterilised by γ radiation at 25 kGy. The CPC used in this study was prepared by mixing MCPM and β -TCP at a ratio of 45 : 55. The mixture was mixed with citric acid with a weight ratio of 80 : 1. Before implantation, the mixture of CPC was mixed with 2% sodium hyaluronate (dissolved in distilled water). Subsequently, the mixture was incorporated with oil-based suspension with or without palm tocotrienol at an oil-to-powder ratio of 0.35 g/g. The ingredient composition was based on a previous study by Luo *et al.* reporting a ready-to-use calcium phosphate paste incorporating an oil suspension, demonstrating good injectability and adequate shelf life [31]. The tocotrienol isolated from *Elaeis guineensis* (batch number: 19060070A0) used in this study was gifted by Davos Life Science Sdn. Bhd. (Selangor, Malaysia). It consists of 28.3% α -tocopherol, 26.8% α -tocotrienol, 2.3% β -tocotrienol, 29.5% γ -tocotrienol, 8.3% δ -tocotrienol, and 4.6% α -tocomonoenol.

Study design

All experimental protocols were evaluated and approved by the Universiti Kebangsaan Malaysia Animals Ethics Committee (UKMAEC) (approval code: FAR/FP/2020/WONG SOK KUAN/22-JULY/1112-OCT-2020-SEP-2022). The timeline of experimental protocols is depicted in Figure 1 A. Twelve-week-old female Sprague-Dawley rats were procured from the Laboratory Animal Resource Unit (LARU), Universiti Kebangsaan Malaysia (Kuala Lumpur, Malaysia). The animals were randomly assigned to four experimental groups: (a) sham-operated controls (sham); (b) ovariectomised rats (OVX);

(c) ovariectomised rats with bone defects implanted with CPC (OVX + CPC); (d) ovariectomised rats with bone defects implanted with palm tocotrienol-doped CPC (OVX + CPC/T3). All rats were housed in individual cages with an ambient temperature of $25 \pm 2^\circ\text{C}$ and an alternated 12-hour light/dark cycle at the animal laboratory, Department of Pharmacology, Faculty of Medicine, Universiti Kebangsaan Malaysia (Kuala Lumpur, Malaysia). The rats were provided with standard rat chow (Gold Coin, Malaysia) and tap water *ad libitum*. The rats were acclimatised for 1 week before surgery. All surgical procedures were conducted under anaesthesia using 100 mg/kg ketamine and 10 mg/kg xylazine, given via intraperitoneal injection. For the sham-operated controls, the rats were subjected to laparotomy and their ovaries were retained. The remaining groups were subjected to bilateral ovariectomy mimicking a model of postmenopausal osteoporosis in humans. After 11 weeks of ovariectomy, bone defects were created in the OVX + CPC and OVX + CPC/T3 groups, while the sham and OVX groups were subjected to surgical stress. A bone defect (2 mm in diameter and 2 mm in depth) was made 5 mm below the left knee joint using a 2 mm wood drill (Figure 1 B). The freshly prepared treatment material (CPC with or without palm tocotrienol) was gradually added until the bone defect cavity was filled and the cement had hardened. Following surgery, Baytril® (enrofloxacin, 5 mg/kg daily for 5 days) were administered intramuscularly as an antibiotic to prevent infections. For pain management, tramadol (25 mg/kg daily for 5 days) was intramuscularly injected after surgery. Iodine solution was applied to the site as a post-operative antiseptic. Post-operative monitoring was conducted daily to assess wound healing, signs of infection, distress, and overall well-being. The rats were sacrificed using an overdose of ketamine-xylazine

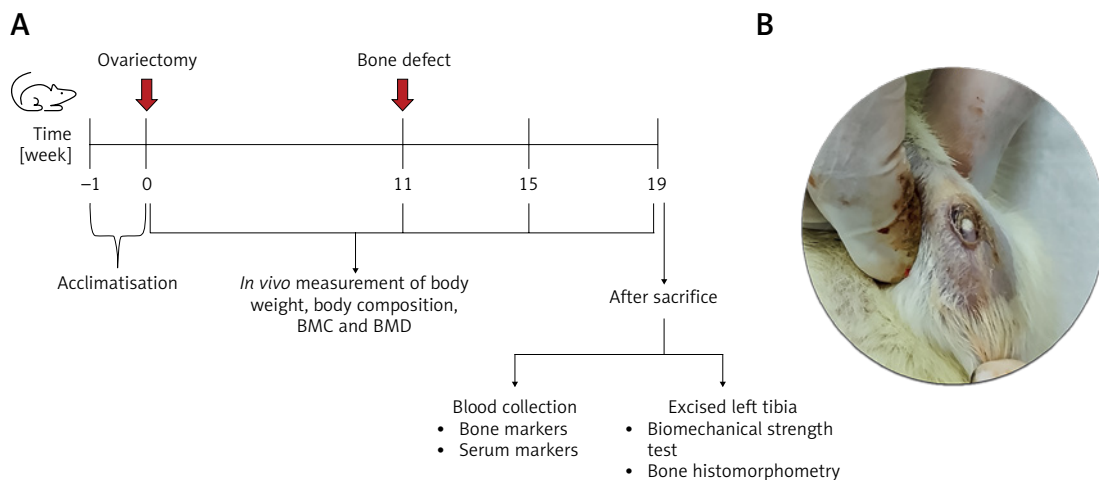


Figure 1. A – Timeline represents the experimental protocol utilised in the present study. **B** – A bone defect (diameter: 2 mm; depth: 2 mm) was created 5 mm below the left knee joint using a wood drill (diameter: 2 mm). The treatment material (CPC with or without palm tocotrienol) was inserted into the bone defect cavity until it was filled completely and the cement had hardened

combination (300 mg/kg ketamine and 30 mg/kg xylazine) 8 weeks after implantation. Blood was collected and left tibias were harvested for analysis.

Sample size calculation

A power analysis was conducted using G*Power software to ensure adequate power for detecting significant differences between groups. The calculation was based on trabecular bone volume (BV/TV) as the primary outcome, referencing from preliminary data. The inputs were: mean (group 1 = 35.96; group 2 = 22.58), standard deviation (group 1 = 3.14; group 2 = 1.90), effect size (5.156), significance level (0.05), power (0.8) and N1/N2 ratio (1). Based on this calculation, a minimum of 6 animals per group was required to detect statistically significant differences, and this was approved by the animal ethics review board.

Measurements of body weight, body composition, bone mineral content (BMC) and bone mineral density (BMD)

The body weight, body composition, BMC, and BMD of the rats were recorded prior to the ovariectomy procedure (week 0), before bone defect creation (week 11), and after the implantation of treatment materials (week 15 and 19). Body weight was measured using a weighing scale. All rats were maintained in the ventral recumbency position on the scanning table under general anaesthesia via intraperitoneal injection (100 mg/kg ketamine and 10 mg/kg xylazine). Whole-body and high-resolution scans were performed to measure body composition, BMC, and BMD using a dual-energy X-ray absorptiometer (DXA) (Hologic QDR-1000 System, Hologic Inc., Waltham, USA).

Bone histomorphometry

Left tibias were fixed in 15% formaldehyde. Half of the tibias were decalcified in ethylenediaminetetraacetic acid (EDTA) solution for 2 months, while the other half of the tibias were left undecalcified. Both parts were dehydrated with a series of ethanol solutions of increasing concentrations. After that, the decalcified part was paraffinised and the undecalcified part was embedded in polymerised resin. Using a micro-

tome, the decalcified bone was sectioned into 5 µm slices and the undecalcified bone into 7 µm slices (Leica RM2235, USA).

The decalcified sections were stained using haematoxylin and eosin (Leica, United State of America) and Masson's trichrome (Bio Optica, Italy) staining kits. Both stained sections were observed under a light microscope equipped with ZEN Microscopy 2.6 software (ZEISS, Germany) with magnifications of 400× and 40×, respectively. Static bone histomorphometry parameters were calculated using the Weibel grid method based on interactions between lines or points of surface measurement on the haematoxylin and eosin staining images. The parameters were osteoblast surface/bone surface (OB/BS, unit = %), osteoclast surface/bone surface (OC/BS, unit = %), eroded surface/bone surface (ES/BS, unit = %), osteoid surface/bone surface (OS/BS, unit = %) and osteoid volume/bone volume (OV/BV, unit = %). The presence of haematopoietic cells, collagen, and trabecular bone at the defect site was graded semi-quantitatively in a blinded manner by an anatomist with expertise in bone histomorphometry to ensure consistency and minimise subjective bias. Established scoring criteria were used to maintain accuracy and reproducibility (Table I) [32, 33].

The undecalcified sections were used for von Kossa staining. The structural bone histomorphometry parameters were observed under a light microscope equipped with CellSens Standard software (Olympus, Japan) at a magnification of 400×. The structural bone histomorphometry parameters were measured using the Fiji image analysis software [34]. The parameters obtained were BV/TV (unit = %), trabecular thickness (Tb.Th, unit = mm), trabecular number (Tb.N, unit = mm⁻¹), and trabecular separation (Tb.Sp, unit = mm).

Measurement of bone biomarkers

The blood samples were immediately processed into serum after collection from the rats, centrifuged at 3,000 rpm for 10 min, and stored at -70°C until analysis. The left tibia was cut (approximately 17 mm from the proximal end of the tibia) and weighed. The bone was cleaned with phosphate-buffered saline to remove red blood cells and clotted blood. The bone was then

Table I. Semi-quantitative assessment scale for the presence of haematopoietic cells, collagen, and trabecular bone at the defect site

Score	Extent of the presence
0	None
1	Scant (less than one-fourth of the area surrounding the defect)
2	Moderate (more than one-fourth and less than one-half of the area surrounding the defect)
3	Abundant (more than one-half of the area surrounding the defect)

crushed using a mortar and pestle in the presence of liquid nitrogen. The samples were homogenised on ice in radioimmunoprecipitation assay buffer containing 50 mM Tris (pH 7.4), 150 mM sodium chloride, 1% Triton X-100, 1% sodium deoxycholate, 1 mM EDTA, 0.1% sodium dodecyl sulphate with the addition of protease (phenylmethylsulfonyl fluoride) and phosphatase (sodium fluoride and sodium orthovanadate) inhibitors (catalogue number: E-BC-R327; Elabscience Biotechnology Inc., China). The sample tube was vortexed, left on ice for 30 min, and centrifuged using a Microfuge 22R centrifuge machine (Beckman Coulter, USA) at 12,000 rpm for 10 min at 4°C. The supernatant was collected and stored at -70°C until analysis.

The levels of bone morphogenetic protein-2 (BMP-2) (catalogue number: E-EL-R0002; Elabscience Biotechnology Inc., China), Runt-related transcription factor 2 (Runx-2) (catalogue number: ELK8429, ELK Biotechnology, China) and osteocalcin (OCN) (catalogue number: E-EL-R0243; Elabscience Biotechnology Inc., China) in bone and serum were measured using enzyme-linked immunosorbent assay kits according to the protocol provided by the supplier. Protein concentrations of bone samples were measured using the Bradford method (Quick Start Bradford Protein Assay, Bio-Rad Laboratories Inc., CA, USA).

Measurements of bone biomechanical strength

The tibiae were cleaned of soft tissues, wrapped in gauze moistened with phosphate-buffered saline, and kept at -80°C upon sacrifice until analysis to prevent false negative results caused by dry and brittle bones that are prone to breaking when load is applied. Bone biomechanical strength test was conducted using a universal testing machine (Autograph AGS-X 500N, Shimadzu, Kyoto, Japan). The three-point bending test was initiated by placing the metaphyseal part of the tibia on an aluminium support with a groove. In contrast, the distal diaphyseal part was placed on an aluminium support without a groove. A load (speed: 1 mm/min) was applied to the tibia in the metaphyseal region until it fractured. Trapezium Lite X software (Shimadzu, Kyoto, Japan) was used to obtain load (unit = N), displacement (unit = mm), stress (unit = N/mm²), and strain (unit = %). A load-displacement graph was plotted, and the slope of the curve was obtained as stiffness (unit = N/mm). A stress-strain graph was plotted, and the slope of the curve was used to define Young's modulus of elasticity (unit = N/mm²).

Statistical analysis

All data were analysed using Statistical Package for the Social Sciences (SPSS) version 24 (IBM,

Armonk, USA). The normality of data was assessed using the Shapiro-Wilk test. The comparison of normally distributed data between groups (for biomechanical strength, bone markers, static and structural bone histomorphometric parameters) was performed using one-way analysis of variance (ANOVA), followed by Tukey's or Dunnett's post hoc test, depending on the homogeneity of variance using Levene's test. For data with multiple time intervals (including body weight, lean mass, fat mass, BMC and BMD), the comparisons between groups were performed using mixed-design ANOVA with small effect analysis. All normally distributed data are reported as mean ± standard error of the mean (SEM). Discrete data obtained from histomorphometry analysis (including the presence of haematopoietic cells, collagen, and trabecular bone) are presented as median ± interquartile range and were analysed using the Mann-Whitney *U* test. Statistical significance was set at $p < 0.05$.

Results

Effects of CPC and CPC/T3 implantation on body weight and body composition of ovariectomised rats with bone defects

The body weight of rats in all experimental groups increased significantly at weeks 11, 15, and 19 as compared to week 0 ($p < 0.05$). The OVX and OVX + CPC/T3 groups showed a significant increase in body weight at weeks 15 and 19 compared to week 11 ($p < 0.05$). A significant increase in body weight was observed in the OVX + CPC group at week 19 compared to week 11 ($p < 0.05$). The OVX, OVX + CPC, and OVX + CPC/T3 groups showed a significant increase in body weight at week 19 compared to week 15 ($p < 0.05$). For between-group comparisons, a significant increase in body weight was observed in the OVX, OVX + CPC, and OVX + CPC/T3 groups compared to the sham group at weeks 11, 15, and 19 ($p < 0.05$). The OVX + CPC and OVX + CPC/T3 groups showed a significant increase in body weight compared to the OVX group at week 15 ($p < 0.05$) (Table II A).

The lean mass of rats of the sham group at weeks 15 and 19 was significantly higher than week 0 ($p < 0.05$). The OVX, OVX + CPC, and OVX + CPC/T3 groups showed increased lean mass at weeks 11, 15, and 19 compared to week 0 ($p < 0.05$). For between-group comparisons, the OVX + CPC/T3 group had significantly higher lean mass than the sham group at weeks 15 and 19 ($p < 0.05$) (Table II B).

The fat mass of rats in all groups was significantly higher at weeks 11, 15, and 19 compared to week 0 ($p < 0.05$). The OVX, OVX + CPC, and OVX + CPC/T3 groups showed a significant increase in

Table II. Effects of CPC and CPC/T3 implantation on body weight, lean mass, and fat mass in ovariectomised rats with bone defects at weeks 0, 11, 15, and 19

Parameter	Week 0	Week 11	Week 15	Week 19
A Body weight [g]				
Sham	206.67 ±3.28	251.55 ±5.20*	256.43 ±4.86*	260.97 ±4.52*
OVX	213.78 ±1.16	302.12 ±3.88 ^{a,*}	324.05 ±4.91 ^{a,*,#}	334.72 ±5.02 ^{a,*,#,@}
OVX + CPC	214.02 ±4.65	298.27 ±6.14 ^{a,*}	305.03 ±5.34 ^{a,b,*}	323.07 ±2.61 ^{a,*,#,@}
OVX + CPC/T3	213.63 ±1.38	297.50 ±7.18 ^{a,*}	310.88 ±2.86 ^{a,b,*,#}	328.42 ±4.17 ^{a,*,#,@}
B Lean mass [g]				
Sham	194.17 ±1.54	213.30 ±8.82	222.19 ±4.36*	222.68 ±6.42*
OVX	195.46 ±1.10	227.69 ±12.73*	243.69 ±12.46*	233.95 ±14.25*
OVX + CPC	195.23 ±3.57	254.03 ±8.93*	250.87 ±6.16*	255.92 ±5.52*
OVX + CPC/T3	190.84 ±1.27	254.18 ±12.17*	274.08 ±8.24 ^{a,*}	276.83 ±6.11 ^{a,*}
C Fat mass [g]				
Sham	23.10 ±4.19	37.90 ±6.39*	40.17 ±8.37*	47.92 ±7.74*
OVX	12.75 ±1.28	29.52 ±3.47*	36.78 ±2.95*	66.35 ±3.74 ^{*,#,@}
OVX + CPC	18.42 ±2.29	37.4 ±4.40*	41.52 ±3.39*	57.75 ±2.38 ^{*,#,@}
OVX + CPC/T3	17.78 ±2.57	42.72 ±5.66*	43.8 ±6.12*	59.63 ±1.09 ^{*,#,@}

Data are expressed as mean ± SEM. Notes: 'a' indicates a significant difference compared to the sham group ($p < 0.05$), 'b' indicates a significant difference compared to the OVX group ($p < 0.05$), '*' indicates a significant difference compared to week 0 ($p < 0.05$), '#' indicates a significant difference compared to week 11 ($p < 0.05$), '@' indicates a significant difference compared to week 15 ($p < 0.05$).

Table III. Effects of CPC and CPC/T3 implantation on whole-body and left tibia BMC and BMD in ovariectomised rats with bone defects at weeks 0, 11, 15, and 19

Parameter	Week 0	Week 11	Week 15	Week 19
A Whole-body BMC [g]				
Sham	7.00 ±0.02	8.65 ±0.14*	8.54 ±0.18*	8.80 ±0.23*
OVX	7.28 ±0.10	9.61 ±0.15 ^{a,*}	10.25 ±0.21 ^{a,*,#}	10.24 ±0.14 ^{a,*,#}
OVX + CPC	7.41 ±0.18	10.31 ±0.13 ^{a,b,*}	10.36 ±0.11 ^{a,*}	10.89 ±0.07 ^{a,b,*,#,@}
OVX + CPC/T3	7.45 ±0.13	10.45 ±0.12 ^{a,b,*}	10.52 ±0.08 ^{a,*}	11.26 ±0.07 ^{a,b,*,#,@}
B Whole-body BMD [g/cm²]				
Sham	0.144 ±0.002	0.167 ±0.002*	0.172 ±0.003*	0.173 ±0.004*
OVX	0.151 ±0.004	0.177 ±0.005*	0.177 ±0.003*	0.180 ±0.003*
OVX + CPC	0.153 ±0.001	0.175 ±0.003*	0.180 ±0.003*	0.181 ±0.002*
OVX + CPC/T3	0.148 ±0.002	0.175 ±0.003*	0.182 ±0.003 ^{*,#}	0.184 ±0.002 ^{*,#}
C Left tibia BMC [g]				
Sham	0.255 ±0.009	0.330 ±0.012*	0.340 ±0.011*	0.335 ±0.010*
OVX	0.238 ±0.007	0.335 ±0.006*	0.335 ±0.014*	0.332 ±0.012*
OVX + CPC	0.237 ±0.013	0.308 ±0.016*	0.343 ±0.022 ^{*,#}	0.350 ±0.023 ^{*,#}
OVX + CPC/T3	0.245 ±0.012	0.313 ±0.020*	0.343 ±0.016 ^{*,#}	0.352 ±0.014 ^{*,#}
D Left tibia BMD [g/cm²]				
Sham	0.172 ±0.007	0.208 ±0.007*	0.209 ±0.008*	0.209 ±0.007*
OVX	0.181 ±0.003	0.205 ±0.002*	0.212 ±0.004*	0.211 ±0.004*
OVX + CPC	0.184 ±0.007	0.205 ±0.009*	0.210 ±0.007*	0.218 ±0.009*
OVX + CPC/T3	0.181 ±0.002	0.200 ±0.006*	0.212 ±0.005*	0.208 ±0.005*

Data are expressed as mean ± SEM. Notes: 'a' indicates a significant difference compared to the sham group ($p < 0.05$), 'b' indicates a significant difference compared to the OVX group ($p < 0.05$), '*' indicates a significant difference compared to week 0 ($p < 0.05$), '#' indicates a significant difference compared to week 11 ($p < 0.05$), '@' indicates a significant difference compared to week 15 ($p < 0.05$).

fat mass at week 19 as compared to weeks 11 and 15 ($p < 0.05$). However, the fat mass of the rats showed no difference between groups throughout the study ($p > 0.05$) (Table II C).

Effects of CPC and CPC/T3 implantation on whole-body and left tibia BMC and BMD of ovariectomised rats with bone defects

The whole-body BMC increased significantly at weeks 11, 15, and 19 as compared to week 0 in all experimental groups ($p < 0.05$). The OVX group showed a significant increase in whole-body BMC at weeks 15 and 19 compared to week 11 ($p < 0.05$). The OVX + CPC and OVX + CPC/T3 groups showed a significantly higher whole-body BMC at week 19 as compared to weeks 11 and 15 ($p < 0.05$). The between-group comparison showed significantly higher whole-body BMC in the OVX, OVX + CPC, and OVX + CPC/T3 groups as compared to the sham group from week 11 to 19 ($p < 0.05$). The OVX + CPC and OVX + CPC/T3 groups showed a significant increase in whole-body BMC compared to the OVX group at weeks 11 and 19 ($p < 0.05$) (Table III A).

The whole-body BMD for all groups increased significantly at weeks 11, 15, and 19 as compared to week 0 ($p < 0.05$). The whole-body BMD of the OVX + CPC/T3 group showed a significant increase at weeks 15 and 19 as compared to week 11 ($p < 0.05$). However, no significant difference was ob-

served for the whole-body BMD between groups throughout the study ($p > 0.05$) (Table III B).

The left tibial BMC and BMD for all groups showed significant increases at week 11, 15, and 19 as compared to week 0 ($p < 0.05$). The OVX + CPC and OVX + CPC/T3 groups showed significant increases in left tibial BMC at weeks 15 and 19 as compared to week 11 ($p < 0.05$). However, left tibia BMC and BMD showed no significant difference between groups throughout the study ($p > 0.05$) (Table III C, D).

Effects of CPC and CPC/T3 implantation on bone histomorphometry of ovariectomised rats with bone defects

Static bone histomorphometry showed that the osteoclast surface (OC/BS) of the OVX + CPC/T3 group was significantly reduced compared to the sham and OVX groups ($p < 0.05$). On the other hand, the OVX + CPC/T3 group had a significantly higher eroded surface (ES/BS) compared to the OVX group ($p < 0.05$). Meanwhile, OB/BS, OS/BS, and OV/BV showed no significant difference between groups ($p > 0.05$) (Figure 2). Representative images of the trabecular bone stained by haematoxylin and eosin are illustrated in Figure 3. Osteoblast and osteoclast cells were stained purple whereas the trabecular bone was stained pink.

There was no significant difference in the presence of haematopoietic cells at the tibial defect

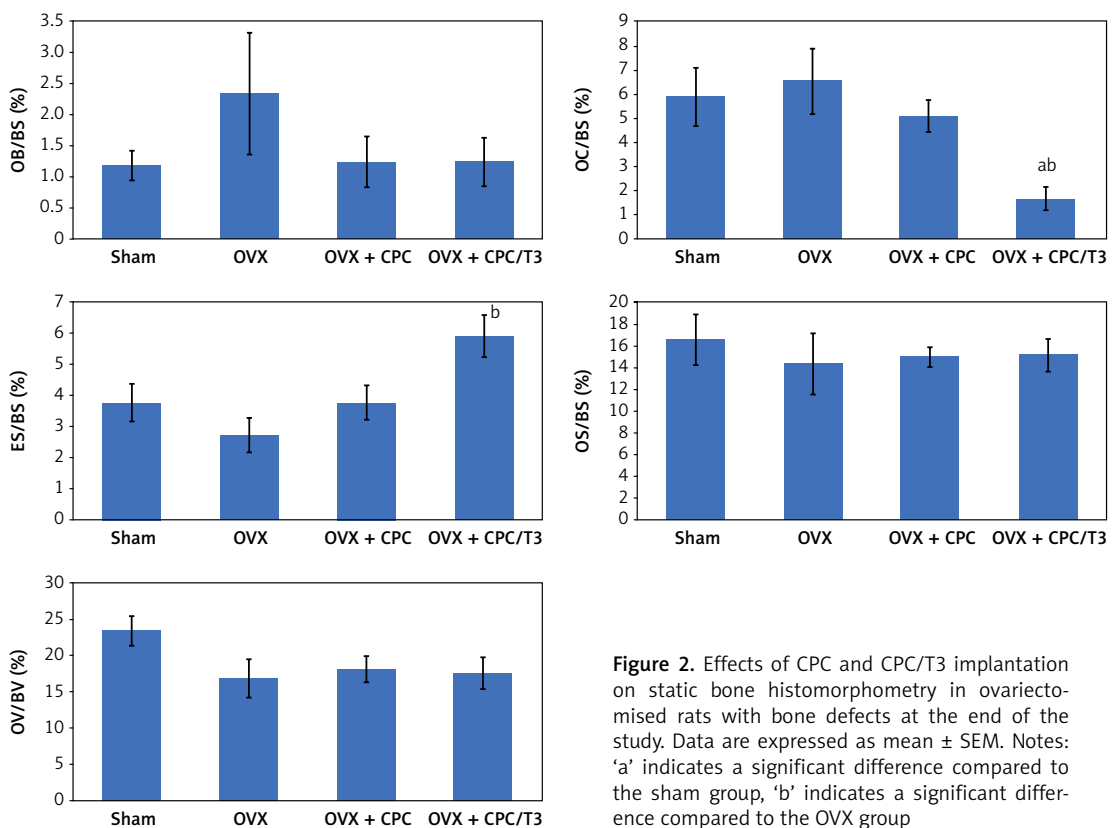


Figure 2. Effects of CPC and CPC/T3 implantation on static bone histomorphometry in ovariectomised rats with bone defects at the end of the study. Data are expressed as mean \pm SEM. Notes: 'a' indicates a significant difference compared to the sham group, 'b' indicates a significant difference compared to the OVX group

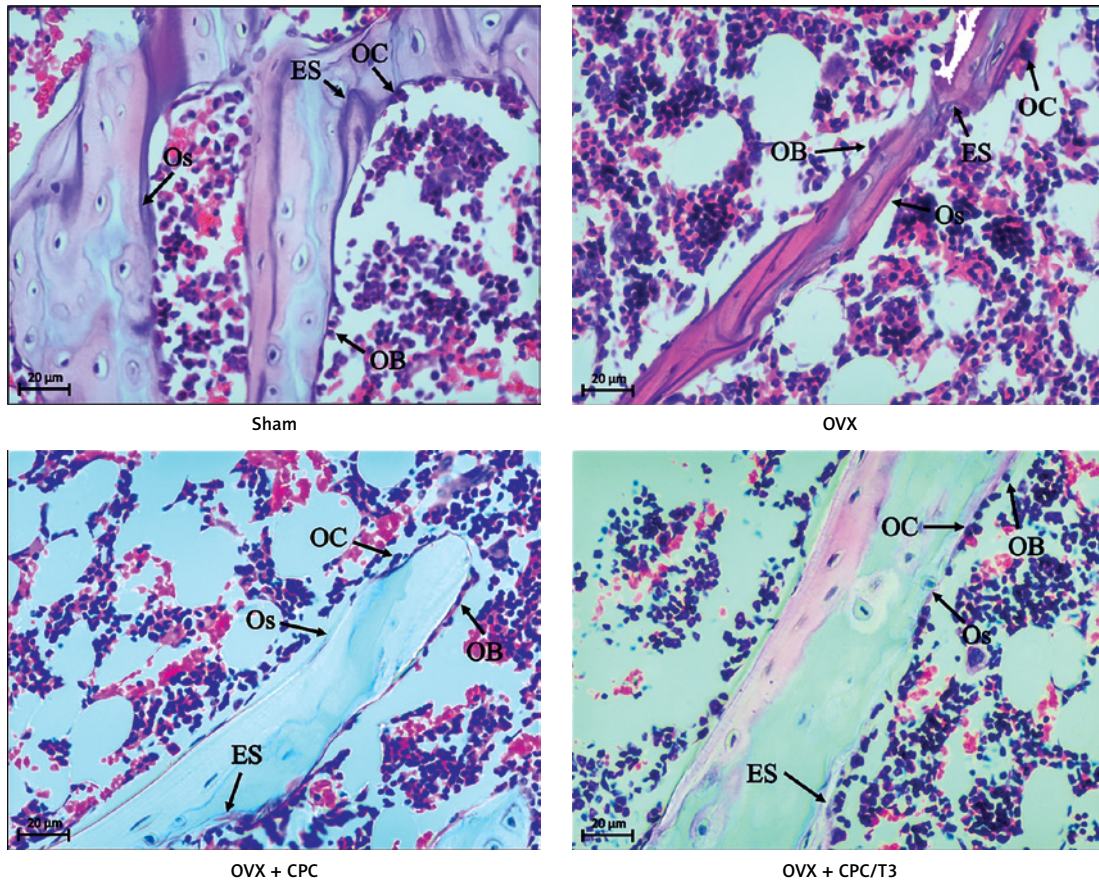


Figure 3. Haematoxylin and eosin staining of tibial trabecular bone in ovariectomised rats at 400× magnification. Notes: 'ES' indicates the eroded surface, 'Os' indicates the osteoid surface, 'OB' indicates the osteoblast surface, 'OC' indicates the osteoclast surface

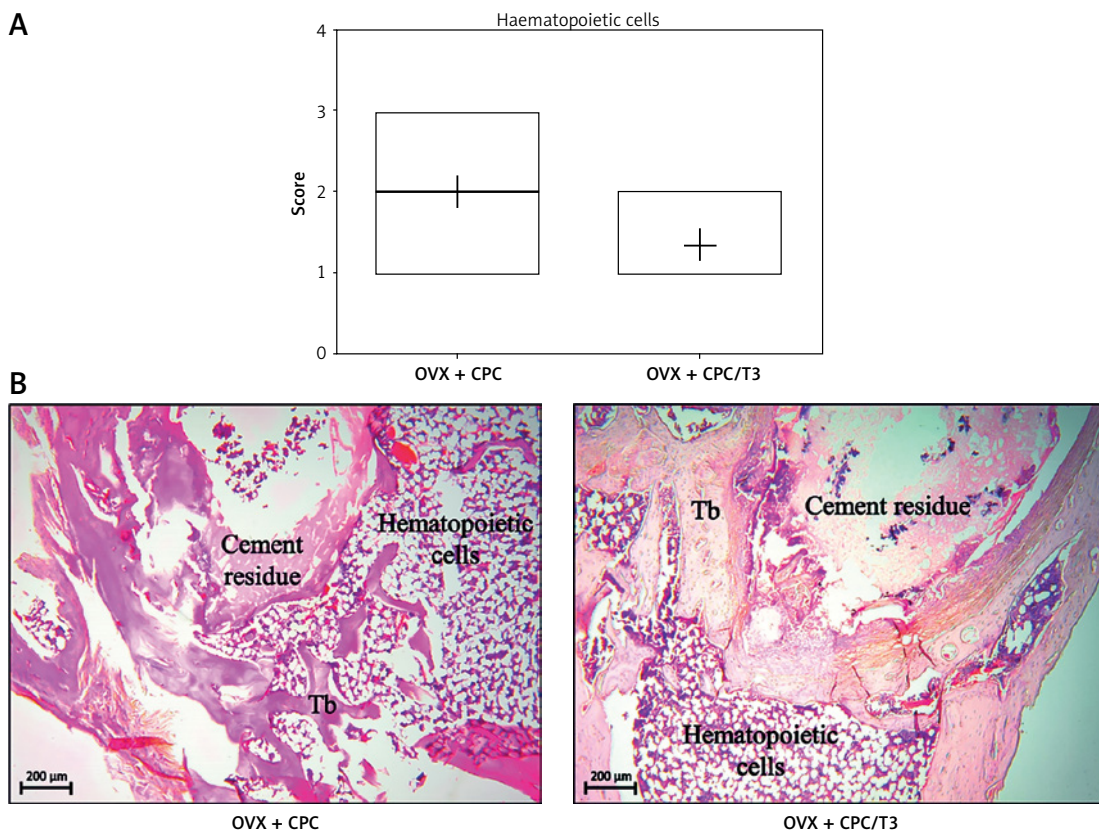


Figure 4. A – Presence of haematopoietic cells at the tibial defect site of rats at the end of the study. **B** – Haematoxylin and eosin staining of the left tibial defect site in ovariectomised rats at 40× magnification. Data are presented as median ± interquartile range. Notes: '+' in the boxplot represents the mean, 'Tb' indicates trabecular bone

site of ovariectomised rats implanted with CPC and CPC/T3 ($p > 0.05$). Haematopoietic cells were stained purple and pink but are located outside the trabecular area (Figure 4).

Masson's trichrome staining showed that the presence of collagen and trabecular bone in the OVX + CPC/T3 group was significantly higher than that in the OVX + CPC group ($p < 0.05$) (Figure 5 A). Representative Masson's trichrome staining images of the left tibial bone defect in ovariectomised rats are illustrated in Figure 5 B. Collagen was stained blue, trabeculae were stained red, and cement residues were stained pink.

Structural histomorphometry indicated that BV/TV was significantly lower in the OVX group than the sham group ($p < 0.05$). The OVX + CPC/T3 group exhibited higher BV/TV than the OVX group ($p < 0.05$). Tb.Th, Tb.N, and Tb.Sp showed no difference between the groups ($p > 0.05$) (Figure 6). Representative von Kossa staining images of the left tibial in ovariectomised rats are illustrated in Figure 7. The trabecular bone appeared brown, and darker staining indicated higher calcium deposition.

Effects of OVX + CPC and OVX + CPC/T3 implantation on bone biomarkers expressed in ovariectomised rats with bone defects

In bone, the BMP-2 level in the OVX + CPC/T3 group was significantly higher compared to the sham, OVX, and OVX + CPC groups ($p < 0.05$). The level of Runx-2 in the OVX+CPC/T3 group was significantly higher than in the OVX and CPC groups ($p < 0.05$). There was no difference in the OCN expression among all the experimental groups ($p > 0.05$) (Figure 8 A). In serum, significantly lower levels of BMP-2 and OCN were noted in the OVX + CPC/T3 group relative to the OVX group ($p < 0.05$). However, the Runx-2 expression did not differ between the groups ($p > 0.05$) (Figure 8 B).

Effects of CPC and CPC/T3 implantation on bone biomechanical strength of ovariectomised rats with bone defects

The left tibia of the OVX + CPC/T3 group had significantly higher stiffness compared to the sham and OVX groups ($p < 0.05$). However, no sig-

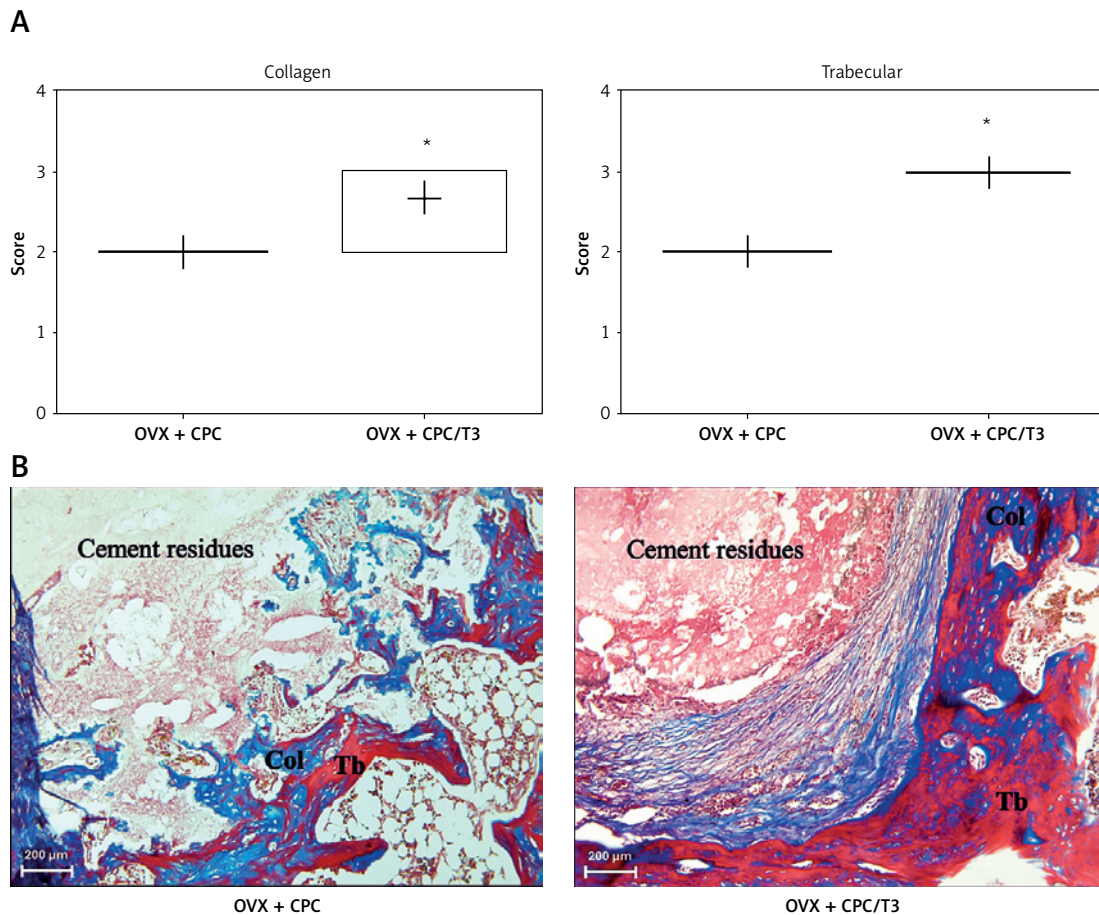


Figure 5. A – Presence of collagen and trabecular bone at the tibial defect site of rats at the end of the study. **B** – Masson's trichrome staining of the left tibial defect site in ovariectomised rats at 40 \times magnification. Data are presented as median \pm interquartile range. Notes: '+' in the boxplot represents the mean value, '*' indicates significant difference compared to the OVX+CPC group, 'Tb' indicates trabecular bone, 'Col' indicates collagen

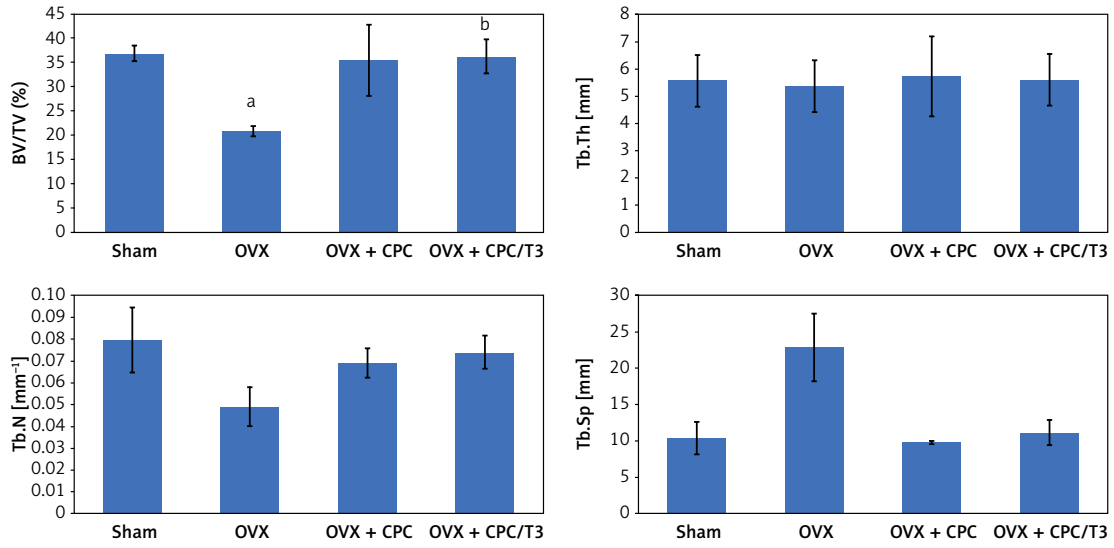


Figure 6. Effects of CPC and CPC/T3 implantation on structural bone histomorphometry in ovariectomised rats with bone defects at the end of the study. Data are expressed as mean \pm SEM. Notes: 'a' indicates a significant difference compared to the sham group, 'b' indicates a significant difference compared to the OVX group

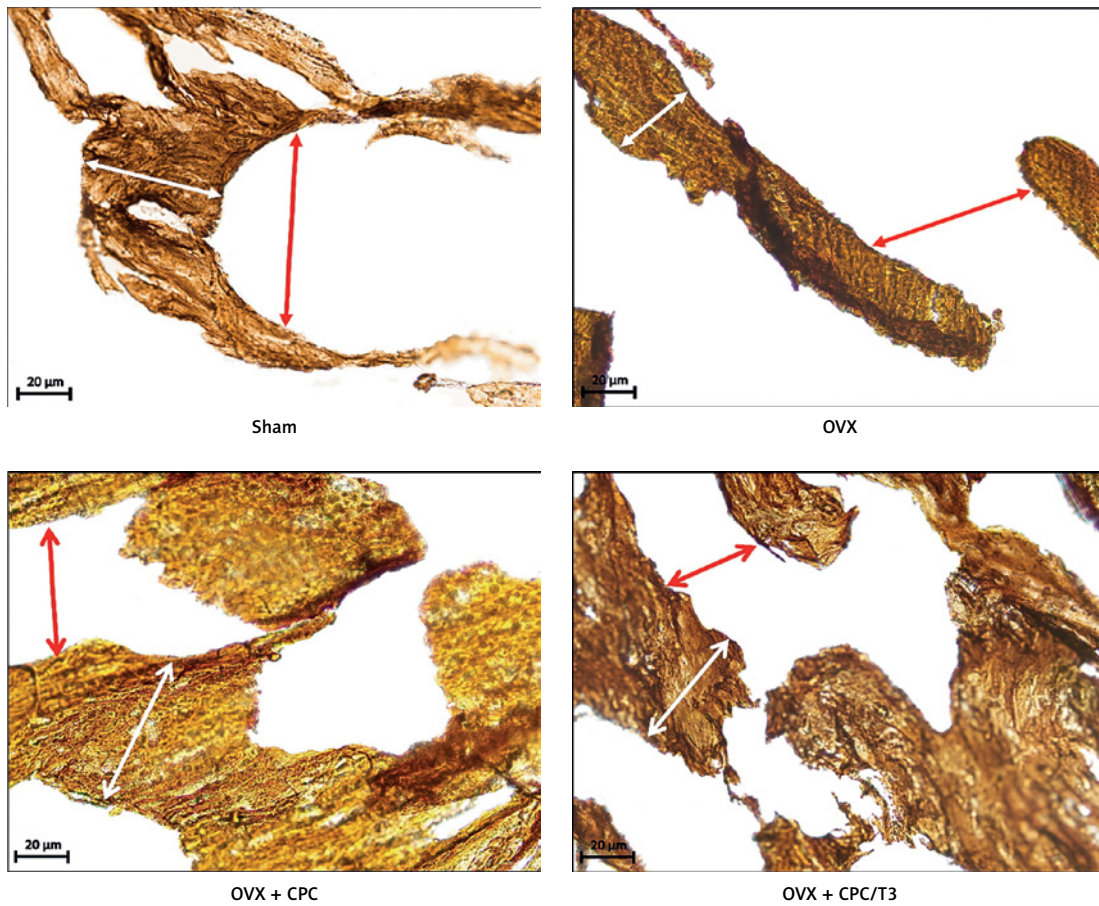


Figure 7. von Kossa staining of the tibial trabecular bone in ovariectomised rats at 400 \times magnification. White arrows indicate trabecular thickness, while red arrows indicate trabecular separation

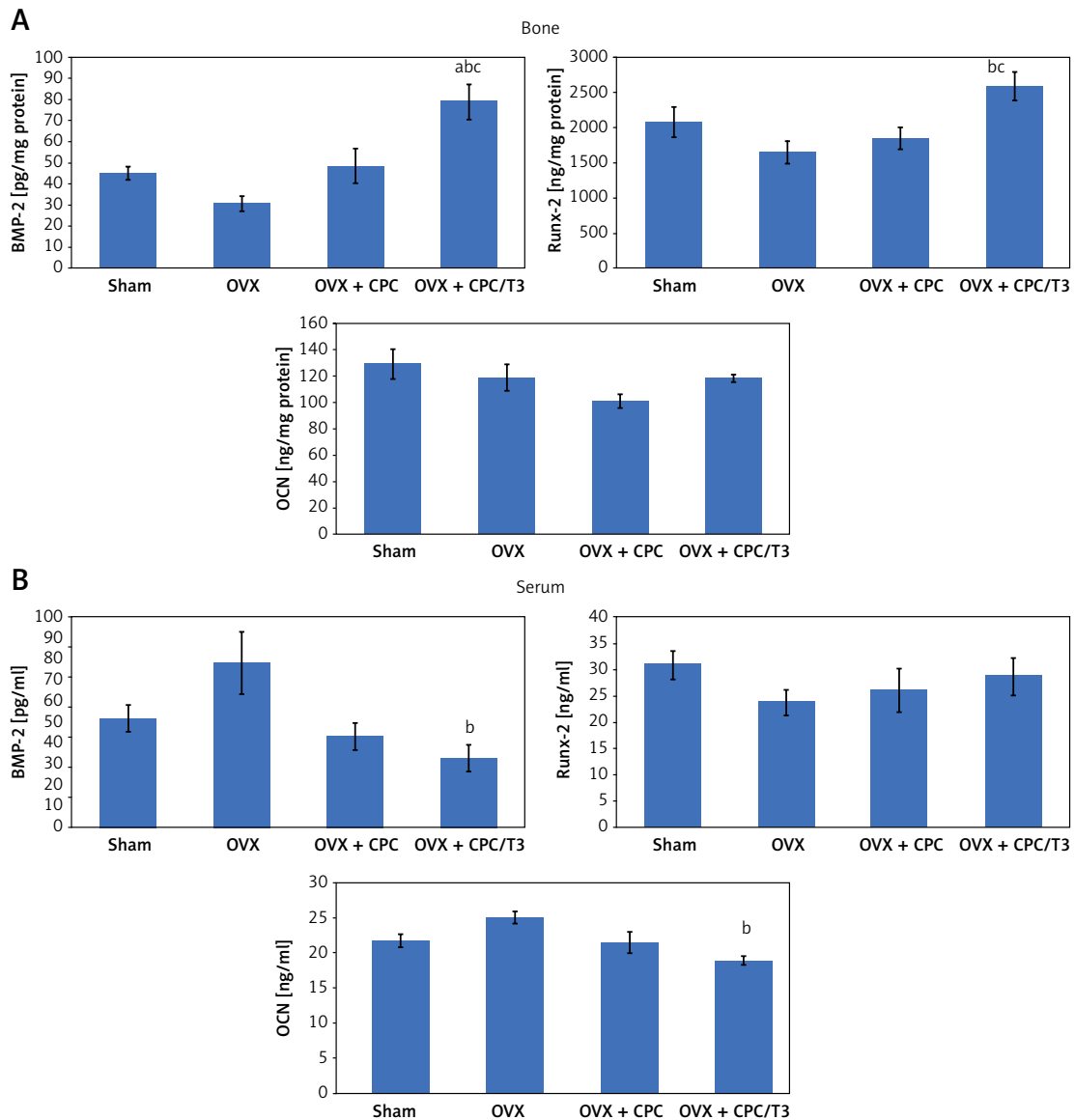


Figure 8. Effects of CPC and CPC/T3 implantation on BMP-2, Runx-2 and OCN expression in (A) bone and (B) serum of the ovariectomised rats with bone defects at the end of the study. Data are expressed as mean \pm SEM. Notes: 'a' indicates a significant difference compared to the sham group, 'b' indicates a significant difference compared to the OVX group, 'c' indicates a significant difference compared to the OVX + CPC group

nificant difference between groups was noted for other bone biomechanical strength parameters ($p > 0.05$) (Figure 9).

Discussion

In this study, implantation of CPC supplemented with tocotrienol increased whole body BMC, stiffness, eroded surface, and bone volume, and decreased osteoclast surface in the ovariectomised rats. Higher expression of BMP-2 and Runx-2 as well as higher formation of collagen and trabecular bone were noted at the defect site of the ovariectomised rats, indicating higher osteogenic capacity of CPC supplemented with tocotrienol than CPC alone. The findings of this study will increase the commercial value of tocotrienol

and improve the application of CPC as a bone substitute to offer an alternative treatment for bone defects in osteoporosis.

In the preparation of CPC mixture with or without palm tocotrienol, citric acid acts as a retardant that prolongs the setting time of the cement [35]. Sodium hyaluronate in distilled water acts as a gel-forming polymer, increasing the viscoelasticity and hydrating properties of CPC paste [26]. Sodium hyaluronate and distilled water should be added immediately after creating the bone defect cavity at the rat's tibia, because the CPC paste hardens within minutes after mixing with sodium hyaluronate and distilled water. Blood oozing from the bone defect cavity due to drilling stops after the paste hardens and fills the cavity.

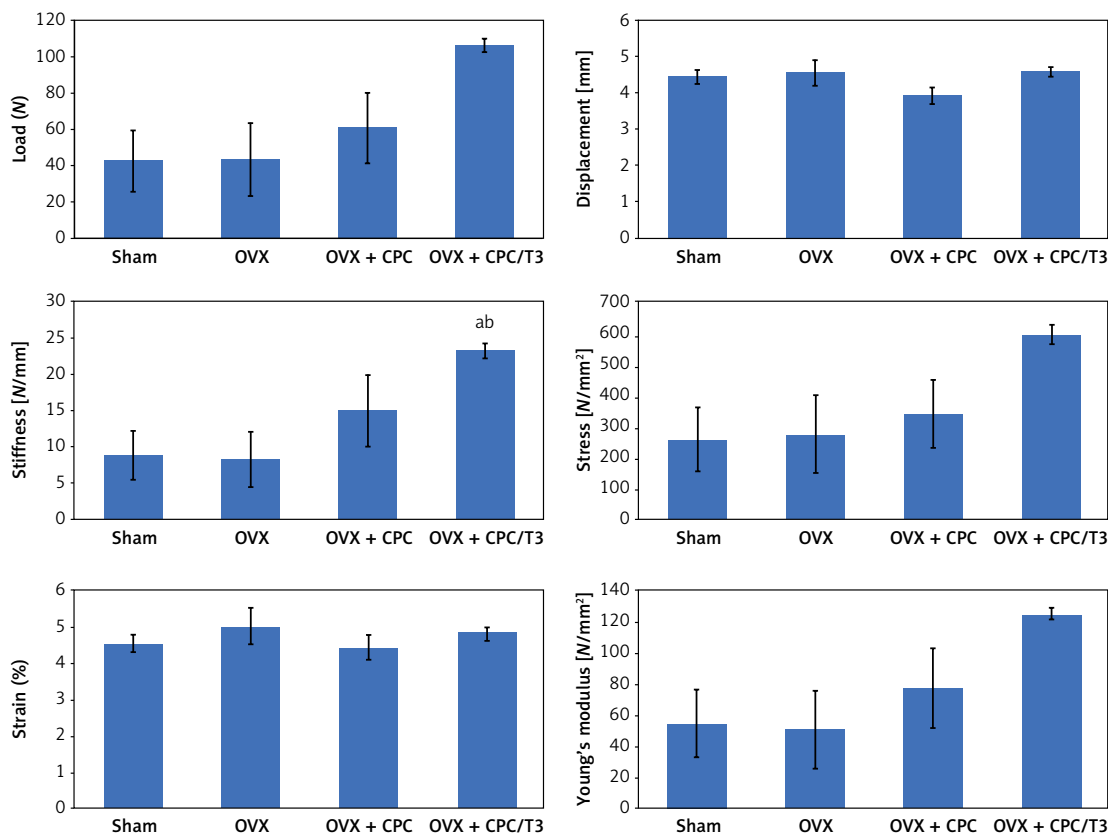


Figure 9. Effects of CPC and CPC/T3 implantation on bone biomechanical strength in the ovariectomised rats with bone defects at the end of the study. Data are expressed as mean \pm SEM. Notes: 'a' indicates a significant difference compared to the sham group, 'b' indicates a significant difference compared to the OVX group

The body weight and fat mass of sham-operated rats increased from the onset of the study to week 11, then plateaued until week 19. Similarly, the lean mass of sham-operated rats increased until week 15 and remained stable until the end of the study. On the other hand, the body weight and fat mass in the OVX, OVX + CPC, and OVX + CPC/T3 groups continued to increase throughout the study period. These observations could be attributed to the increase in food consumption after the ovaries were removed (oestrogen level was decreased), leading to the increase in body weight and fat mass [36, 37]. Our findings were in line with studies by Ekeuku *et al.* and Mohamad *et al.* demonstrating that the rats gained weight after undergoing ovariectomy [22, 38].

In this study, DXA was used to evaluate the impact of CPC with or without tocotrienol on BMC and BMD in the whole body and at the tibial bone defect site in ovariectomised rats. DXA measures bone density using a small dose of ionising radiation [39]. The implantation of CPC and CPC supplemented with tocotrienol increased whole-body BMC compared to the sham and OVX groups. Our findings also indicated that the whole-body BMD continued to increase at week 15 in ovariectomised rats following CPC/T3 implantation,

which was not seen in other experimental groups. After CPC and CPC/T3 implantation, the left tibia BMC in ovariectomised rats also increased at week 15, but these observations were not seen in the sham and OVX groups. The study findings suggested that CPC alone and CPC doped with tocotrienol enhanced whole-body and tibial BMC. The incorporation of tocotrienol offered slight improvement, whereby the whole-body BMD continued to increase at week 15. Tocotrienol can increase the mineral content and density of the bone, augmenting the properties of CPC. Our results are supported by a previous study by Ibrahim *et al.*, which demonstrated that tocotrienol (given through oral administration and intraosseous injection) was effective in preserving bone quality by increasing BMC and BMD in the tibia of ovariectomised rats [40]. Since BMC and BMD are key predictors of fracture risk [41], moderate improvements in BMC and BMD can lead to substantial reductions in fracture incidence in a clinical setting. These findings highlighted the potential clinical relevance of CPC supplemented with tocotrienol as a bone-protective strategy.

Bone histomorphometry is a quantitative analysis used to evaluate bone tissue during the healing process. In static bone histomorphom-

etry, haematoxylin and eosin staining is used to visualise the number and activity of bone cells (osteoblasts and osteoclasts) in response to implanted materials at a specific time point [42, 43]. In this study, the implantation of CPC incorporated with tocotrienol resulted in a decrease in OC/BS but an increase in ES/BS compared to the OVX group. Bone resorption occurs before bone formation during bone remodelling under physiological conditions. The increase in bone resorption might be a result of active osteoclast activity that occurred earlier (after ovariectomy surgery and creation of the bone defect) to absorb bone fragments around the bone defect. After 8 weeks of implantation, the osteoclast count started to decrease, protecting ovariectomised rats against bone loss and initiating bone formation for bone repair. These results were consistent with a study conducted by Abdul-Majeed *et al.* in which the osteoclasts in ovariectomised rats treated with a combination of lovastatin and delta-tocotrienol decreased after 8 weeks of treatment [44]. In other research, ovariectomised rats treated with palm tocotrienol (consisting of 37.2% α -tocotrienol, 39.1% γ -tocotrienol, and 22.6% δ -tocotrienol) had fewer osteoclasts after 4 weeks of treatment [45]. Another study by Mohd Ramli *et al.* found that annatto tocotrienol given orally decreased osteoclast count in adrenalectomised rats after 2 months of treatment [46].

Haematopoietic cells are multipotent cells with the capacity to differentiate into blood cells [47]. Haematopoietic cells can differentiate into osteoclasts to start the bone repair process [48]. At the tibial bone defect site of ovariectomised rats, the incorporation of CPC with tocotrienol did not cause any change in haematopoietic cells between the OVX + CPC and OVX + CPC/T3 groups. To date, research on the effects of tocotrienol on hematopoietic cells in bones is limited.

Masson's trichrome staining is used to differentiate newly deposited bone containing type 1 collagen from older calcified bone [49]. Collagen assembles into fibrils, which are then mineralised into bone via the formation of apatite crystals [50]. The incorporation of CPC with tocotrienol resulted in increased collagen and trabecular bone formation at the tibial bone defect site of ovariectomised rats compared to those implanted with CPC alone. In accordance with the findings of the current study, an earlier study found that application of a tocotrienol-rich fraction increased collagen deposition in skin wounds of mice with type 2 diabetes mellitus [51].

von Kossa staining is a histological technique used to quantify mineralisation (calcium deposits) in bone using two-step reactions. Firstly, silver reacts with phosphate in bone resulting in the for-

mation of transient yellow colouration. Secondly, bound silver is converted to black metallic silver with the aid of light. Thus, bone-containing mineral deposits have a dark brown to black colouration [52]. In this study, BV/TV was lower in the OVX rats compared to the sham group. The ovariectomy-induced reduction in oestrogen production causes a rise in bone resorption and a fall in bone formation, which accelerates the deterioration of the trabecular bone structure. Therefore, the ovariectomy model mimics the pathophysiology of postmenopausal osteoporosis, which delays the healing of bone defects. The results of this investigation were in line with earlier research reporting that the ovariectomised rats exhibited reduced trabecular bone volume as compared to normal rats [22]. In the present study, the implantation of CPC enhanced with tocotrienol into the tibial bone defects increased BV/TV in the ovariectomy rats compared to the OVX group, supporting the view that the presence of tocotrienol slowed down bone loss in ovariectomised rats with bone defects. A study by Ekeuku *et al.* showed that tocotrienol inhibited the decrease in metaphyseal and subchondral femur BV/TV caused by ovariectomy [53].

In this research, the effects of CPC combined with palm tocotrienol on bone markers (such as BMP-2, Runx-2, and OCN) in ovariectomised rats with bone defects were examined. BMP-2 is a transforming growth factor-beta that promotes the differentiation of mesenchymal stem cells into osteoblasts. BMP-2 binds to type I and type II serine/threonine kinase receptors expressed on target cells to phosphorylate downstream Smad proteins. Subsequently, the activated Smad promotes upregulation of Runx-2 and Osterix, leading to expression of alkaline phosphatase (ALP), collagen I, OCN, and osteopontin for bone matrix synthesis [54].

In this study, the results demonstrated that incorporating tocotrienol into CPC enhanced the expression of BMP-2 and Runx-2 but did not affect OCN level in the bone. BMP-2 and Runx2 are early-stage markers of osteogenesis primarily involved in osteoblast differentiation and initiation of bone formation. On the other hand, OCN is a late-stage marker of bone mineralisation, typically expressed at the final stages of osteoblast maturation. The results of the current findings showed that the early stage of osteogenic differentiation was active (as evidenced by BMP-2 and Runx2 upregulation), while the later stage of bone matrix mineralisation had not begun at the time of assessment. Our findings are supported by Chin *et al.*, who reported that BMP-2 level was elevated in ovariectomised rats treated with oral tocotrienol and oral lovastatin [55]. An *in vitro* study

showed that tocotrienol enhanced the expression of BMP-2 in murine pre-osteoblast cells [56]. Prior research revealed that rats subjected to ovariectomy and treated with tocotrienol exhibited higher Runx-2 levels [28]. In nicotine-induced osteoporotic animals, treatment with palm tocotrienol for two months raised the expression of Runx-2 in the femur compared to the negative control group [57]. Research by Mohamad *et al.* also showed that treatment with annatto tocotrienol orally in a rat model of osteoporosis induced by buserelin did not show a significant difference in the expression of OCN after 3 months of treatment [58].

The circulating BMP-2 and OCN levels were decreased in the OVX+CPC/T3 group compared to the OVX group in the current study, indicating increased bone retention of these markers. BMP-2 and OCN have a strong affinity with bone matrix (hydroxyapatite), responsible for bone mineralisation [59, 60]. Thus, the presence of bone defects in osteoporosis is often associated with decreased hydroxyapatite crystal formation, resulting in increases in serum BMP-2 and OCN levels. In a study examining the level of bone turnover markers among osteoporotic and non-osteoporotic patients, Jiang *et al.* reported that patients with osteoporosis had higher levels of OCN and C-telopeptide cross-linked type 1 collagen (β -CTX) in peripheral blood than non-osteoporotic subjects, indicating elevated bone turnover [61].

The bone biomechanical strength test is a useful metric for evaluating a bone's resistance to fracture, determined by load, displacement, stiffness, stress, strain, and Young's modulus of elasticity of the bone. Load, displacement, and stiffness represent extrinsic qualities related to the general composition of the bone. Stress, strain, and Young's modulus of elasticity represent the intrinsic properties associated with the features of bone tissue. Load and stress represent the maximum force required to break a bone. Displacement and strain refer to the degree of deformation when maximum load or stress is applied. Stiffness and Young's modulus of elasticity describe the degree of resistance in a bone towards deformation [62]. The results of this study showed that the bones implanted with CPC supplemented with tocotrienol had higher stiffness than the bones without implantation, indicating that the incorporation of tocotrienol into CPC was required to enhance the bone biomechanical strength at the tibial bone defect site. Comparable studies by Ibrahim *et al.* and Mohamad *et al.* demonstrated that tocotrienol enhanced the femur's biomechanical strength in ovariectomised rats [22, 40]. Additionally, treatment with emulsified palm tocotrienol promotes bone stiffness in the femur of ovariectomised rats [53]. However, other biomechanical parameters

did not show significant differences. The results suggested that CPC with tocotrienol contributed to some structural reinforcement, but its overall biomechanical enhancement might be limited or required a longer duration to observe measurable changes. The improvement in stiffness of the bones implanted with CPC supplemented with tocotrienol might be due to early osteogenic differentiation and better collagen matrix organisation. No significant changes in maximum force, resistance to deformation, and elasticity were observed, as bone mineralisation might take longer to occur and translate into significant biomechanical improvements.

This study effectively demonstrated the potential of tocotrienol-doped CPC in promoting bone regeneration using multiple assessment modalities such as bone densitometry, histological analysis, biochemical markers, and biomechanical testing. These diverse approaches ensure a robust interpretation of the results and strengthen the reliability of the findings, offering a comprehensive evaluation of bone quality, cellular activity and strength. However, this study has several limitations. Firstly, the tocotrienol release rate from CPC was not evaluated, making it unclear how tocotrienol is released from the CPC matrix over time. Without understanding whether tocotrienol is rapidly diffused or released in a sustained manner, its long-term effectiveness in bone healing remains unclear. To address this, *in vitro* drug release studies should be performed using simulated body fluids to analyse the elution profile of tocotrienol over time. High-performance liquid chromatography can be used to quantify tocotrienol release and provide insights into its potential therapeutic efficacy. Secondly, the mechanism of action of tocotrienol in improving the shortcomings of CPC and enhancing bone repair was not studied. Tocotrienol may affect bone metabolism through its potent effects in regulating inflammation, oxidative stress, hormonal changes, and bone peptides [63, 64]. Molecular and cellular analyses, including the profiling of gene expression, oxidative stress markers and inflammatory cytokines, are essential to validate the proposed mechanisms underlying the biological effects of tocotrienol-doped CPC on bone regeneration. Thirdly, the effects of CPC doped with tocotrienol on bone resorption markers were not investigated. Osteoporosis is a systemic skeletal disorder resulting from bone-resorbing activity outweighing bone-forming activity, delaying the bone healing process. Hence, the balance between bone formation and bone resorption activities should be investigated further. Another limitation of this study was the absence of a control group receiving systemic tocotrienol supplementation. Since tocotrienol has

systemic effects on bone metabolism, the absence of a direct comparison makes it unclear whether local application provides a distinct advantage over systemic delivery or if a combination of both approaches would yield superior outcomes.

Several suggestions are recommended to understand the effects of CPC doped with tocotrienol as a bone-repair therapy. It is anticipated that an *in vivo* study with a duration of longer than 8 weeks may result in a rise in bone production, aiding the understanding of the impact of CPC doped with tocotrienol in enhancing bone formation. Bone healing and remodelling are dynamic processes that occur over several months. While an 8-week study may be adequate to assess early-stage bone healing, it may not capture long-term effects such as the mineralisation of newly formed bone, potential degradation of CPC material and late-stage bone cell activities involved in bone remodelling. Furthermore, research with varying tocotrienol concentrations can be conducted to determine the optimal concentration to be incorporated with CPC in promoting bone regeneration. Angiogenesis (the process of new blood vessel formation) is also essential for delivering nutrients and oxygen during bone repair. Research on the angiogenic effects of CPC doped with tocotrienol is recommended to determine its potential in defect site vascularisation, thus suggesting it as a viable approach for accelerated bone regeneration.

While CPC serves as a promising scaffold, the incorporation of tocotrienol introduces bioactive properties that may actively enhance bone regeneration. To establish its clinical application, a direct comparison with other bone grafting approaches (autografts, allografts, synthetic scaffolds and growth factor-based therapies such as BMP-2 or platelet-rich plasma) is necessary. Additionally, regulatory and commercial aspects must be considered, including biocompatibility and toxicity assessments, scalability of production for medical-grade applications, and cost-effectiveness analysis to ensure its viability as a marketable bone graft alternative. Addressing these clinical translation challenges will provide a stronger foundation for the potential use of CPC-tocotrienol in orthopaedic and dental applications, ultimately bringing it closer to clinical application.

In conclusion, the incorporation of palm tocotrienol has the potential to overcome the limitations of CPC, particularly in its mechanical and osteogenic properties. This is evidenced by the implantation of CPC containing palm tocotrienol, which increases bone marker expression, collagen deposition and trabecular bone formation while reducing the number of osteoclasts. These effects contribute to greater stiffness at the bone defect

site of ovariectomised rats. In contrast, CPC alone lacks biomechanical strength and osteogenic capability. Investigating the effects of CPC supplemented with tocotrienol in an established animal model provides valuable translational insights into its potential therapeutic applications for osteoporotic fractures and bone defects in postmenopausal women. CPC enriched with tocotrienol may serve as a scaffold to support bone formation, accelerate healing and improve bone quality in patients with compromised bone healing capacity, highlighting its strong commercialisation potential in orthopaedic and regenerative medicine markets. The positive outcomes obtained from this study await further validation through human trials to explore its clinical applications.

Acknowledgments

We thank Nur Sabariah Adnan, Fadhlullah Zuhair Japar Sidik, Azlan Mohd Arlamsyah, Mohd Mustazil Mohd Noor, Juliana Abdul Hamid, Nurul Hafizah Abas, and Muhammad Iqbal for their technical assistance in this study. We are also grateful for the tocotrienol isolated from *Elaeis guineensis* sponsored by Davos Life Science Sdn. Bhd. (Selangor, Malaysia).

Funding

This work was supported by Universiti Kebangsaan Malaysia (grant number: FF-2024-113).

Ethical approval

Approval number: FAR/FP/2020/WONG SOK KUAN/22-JULY/1112-OCT.-2020-SEP.-2022.

Conflict of interest

The authors declare no conflict of interest.

References

1. Feng X, McDonald JM. Disorders of bone remodeling. *Annu Rev Pathol* 2011; 6: 121-45.
2. Wong SK, Wong YH, Chin KY, Ima-Nirwana S. A review on the enhancement of calcium phosphate cement with biological materials in bone defect healing. *Polymers (Basel)* 2021; 13: 3075.
3. Baker CE, Moore-Lotridge SN, Hysong AA, et al. Bone fracture acute phase response—a unifying theory of fracture repair: clinical and scientific implications. *Clin Rev Bone Miner Metab* 2018; 16: 142-58.
4. Molitoris KH, Huang M, Baht GS. Osteoimmunology of fracture healing. *Curr Osteoporos Rep* 2024; 22: 330-9.
5. Poursmaeili F, Kamalidehghan B, Kamarehei M, Goh YM. A comprehensive overview on osteoporosis and its risk factors. *Ther Clin Risk Manag* 2018; 14: 2029-49.
6. Thormann U, El Khawassna T, Ray S, et al. Differences of bone healing in metaphyseal defect fractures between osteoporotic and physiological bone in rats. *Injury* 2014; 45: 487-93.

7. Kido HW, Bossini PS, Tim CR, et al. Evaluation of the bone healing process in an experimental tibial bone defect model in ovariectomized rats. *Aging Clin Exp Res* 2014; 26: 473-81.
8. Zura R, Braid-Forbes MJ, Jeray K, et al. Bone fracture non-union rate decreases with increasing age: a prospective inception cohort study. *Bone* 2017; 95: 26-32.
9. Zura R, Xiong Z, Einhorn T, et al. Epidemiology of fracture nonunion in 18 human bones. *JAMA Surg* 2016; 151: e162775.
10. Nikolaou VS, Efsthathopoulos N, Kontakis G, Kanakaris NK, Giannoudis PV. The influence of osteoporosis in femoral fracture healing time. *Injury* 2009; 40: 663-8.
11. Salamanca E, Hsu CC, Huang HM, et al. Bone regeneration using a porcine bone substitute collagen composite in vitro and in vivo. *Sci Rep* 2018; 8: 984.
12. Haugen HJ, Lyngstadaas SP, Rossi F, Perale G. Bone grafts: which is the ideal biomaterial? *J Clin Periodontol* 2019; 46 Suppl 21: 92-102.
13. Xue N, Ding X, Huang R, et al. Bone tissue engineering in the treatment of bone defects. *Pharmaceuticals (Basel)* 2022; 15: 879.
14. Sohn HS, Oh JK. Review of bone graft and bone substitutes with an emphasis on fracture surgeries. *Biomater Res* 2019; 23: 9.
15. Xu HHK, Wang P, Wang L, et al. Calcium phosphate cements for bone engineering and their biological properties. *Bone Research* 2017; 5: 17056.
16. Md Dali SS, Wong SK, Chin KY, Ahmad F. The osteogenic properties of calcium phosphate cement doped with synthetic materials: a structured narrative review of preclinical evidence. *Int J Mol Sci* 2023; 24: 7161.
17. Saud Gany SL, Chin KY, Tan JK, Aminuddin A, Makpol S. Preventative and therapeutic potential of tocotrienols on musculoskeletal diseases in ageing. *Front Pharmacol* 2023; 14: 1290721.
18. Qureshi AA, Khan DA, Silswal N, Saleem S, Qureshi N. Evaluation of pharmacokinetics, and bioavailability of higher doses of tocotrienols in healthy fed humans. *J Clin Exp Cardiol* 2016; 7: 434.
19. Nakatomi T, Itaya-Takahashi M, Horikoshi Y, et al. The difference in the cellular uptake of tocopherol and tocotrienol is influenced by their affinities to albumin. *Sci Rep* 2023; 13: 7392.
20. Wong SK, Mohamad NV, Ibrahim N, Chin KY, Shuid AN, Ima-Nirwana S. The molecular mechanism of vitamin E as a bone-protecting agent: a review on current evidence. *Int J Mol Sci* 2019; 20: 1453.
21. Chin KY, Ima-Nirwana S. The biological effects of tocotrienol on bone: a review on evidence from rodent models. *Drug Des Devel Ther* 2015; 9: 2049-61.
22. Mohamad NV, Ima-Nirwana S, Chin KY. Therapeutic potential of annatto tocotrienol with self-emulsifying drug delivery system in a rat model of postmenopausal bone loss. *Biomed Pharmacother* 2021; 137: 111368.
23. Ekeuku SO, Mohd Ramli ES, Abdullah Sani N, Abd Ghafar N, Soelaiman IN, Chin KY. Tocotrienol as a protecting agent against glucocorticoid-induced osteoporosis: a mini review of potential mechanisms. *Molecules* 2022; 27: 5862.
24. Norazlina M, Maizatul-Neza J, Azarina A, Nazrun AS, Norliza M, Ima-Nirwana S. Effects of vitamin E on receptor activator of nuclear factor kappa B ligand (RANKL) and osteoprotegerin (OPG) in rats treated with nicotine. *Med J Malaysia* 2010; 65: 14-7.
25. Wong SK, Chin KY, Suhaimi FH, Ahmad F, Ima-Nirwana S. The effects of vitamin E from *Elaeis guineensis* (Oil Palm) in a rat model of bone loss due to metabolic syndrome. *Int J Environ Res Public Health* 2018; 15: 1828.
26. Wong SK, Chin KY, Suhaimi FH, Ahmad F, Ima-Nirwana S. Exploring the potential of tocotrienol from *Bixa orellana* as a single agent targeting metabolic syndrome and bone loss. *Bone* 2018; 116: 8-21.
27. Mohamad S, Shuid AN, Mokhtar SA, Abdullah S, Soelaiman IN. Tocotrienol supplementation improves late-phase fracture healing compared to alpha-tocopherol in a rat model of postmenopausal osteoporosis: a biomechanical evaluation. *Evid Based Complement Alternat Med* 2012; 2012: 372878.
28. Ibrahim N, Mohamed N, Soelaiman IN, Shuid AN. The effects of targeted deliveries of lovastatin and tocotrienol on ossification-related gene expressions in fracture healing in an osteoporosis rat model. *Int J Environ Res Public Health* 2015; 12: 12958-76.
29. Wong SK, Chin KY, Ahmad F, Ima-Nirwana S. Regulation of inflammatory response and oxidative stress by tocotrienol in a rat model of non-alcoholic fatty liver disease. *J Funct Foods* 2020; 74: 104209.
30. Wong SK, Fikri NIA, Munesveran K, et al. Effects of tocotrienol on osteocyte-mediated phosphate metabolism in high-carbohydrate high-fat diet-induced osteoporotic rats. *J Funct Foods* 2022; 96: 105213.
31. Luo J, Engqvist H, Persson C. A ready-to-use acidic, brushite-forming calcium phosphate cement. *Acta Biomater* 2018; 81: 304-14.
32. Zhu J, Zhang C, Jia J, et al. Osteogenic effects in a rat osteoporosis model and femur defect model by simvastatin microcrystals. *Ann N Y Acad Sci* 2021; 1487: 31-42.
33. Ibrahim N, Mohamed IN, Mohamed N, Mohd Ramli ES, Shuid AN. The effects of aqueous extract of *Labisia pumila* (Blume) Fern.-Vill. Var. *Alata* on wound contraction, hydroxyproline content and histological assessments in superficial partial thickness of second-degree burn model. *Front Pharmacol* 2022; 13: 968664.
34. Schindelin J, Arganda-Carreras I, Frise E, et al. Fiji: an open-source platform for biological-image analysis. *Nat Methods* 2012; 9: 676-682.
35. Mishchenko O, Yanovska A, Kosinov O, et al. Synthetic calcium-phosphate materials for bone grafting. *Polymers (Basel)* 2023; 15: 3822.
36. Leeners B, Geary N, Tobler PN, Asarian L. Ovarian hormones and obesity. *Hum Reprod Update* 2017; 23: 300-21.
37. Chen Y, Heiman ML. Increased weight gain after ovariectomy is not a consequence of leptin resistance. *Am J Physiol Endocrinol Metab* 2001; 280: E315-22.
38. Ekeuku SO, Chin KY, Qian J, et al. Normalisation of high bone remodelling due to oestrogen deficiency by Traditional Chinese Formulation Kang Shuai Lao Pian in ovariectomised rats. *Int J Med Sci* 2022; 19: 1648-59.
39. Holmes CJ, Racette SB. The utility of body composition assessment in nutrition and clinical practice: an overview of current methodology. *Nutrients* 2021; 13: 2493.
40. Ibrahim N, Mohd Noor H, Shuid AN, et al. Osteoprotective effects in postmenopausal osteoporosis rat model: oral tocotrienol vs. intraosseous injection of tocotrienol-poly lactic-co-glycolic acid combination. *Front Pharmacol* 2021; 12: 706747.
41. Curtis EM, Harvey NC, D'Angelo S, et al. Bone mineral content and areal density, but not bone area, predict an incident fracture risk: a comparative study in a UK prospective cohort. *Arch Osteoporos* 2016; 11: 39.
42. Li L, Peng X, Qin Y, et al. Acceleration of bone regeneration by activating Wnt/ β -catenin signalling pathway via

- lithium released from lithium chloride/calcium phosphate cement in osteoporosis. *Sci Rep* 2017; 7: 45204.
43. Saif AM, Norazlina M, Ima-Nirwana S. Quantification of bone histomorphometric parameters using the weibel technique in animals. *Med Health* 2016; 11: 278-88.
 44. Abdul-Majeed S, Mohamed N, Soelaiman IN. Effects of tocotrienol and lovastatin combination on osteoblast and osteoclast activity in estrogen-deficient osteoporosis. *Evid Based Complement Alternat Med* 2012; 2012: 960742.
 45. Muhammad N, Luke DA, Shuid AN, Mohamed N, Soelaiman IN. Two different isomers of vitamin e prevent bone loss in postmenopausal osteoporosis rat model. *Evid Based Complement Alternat Med* 2012; 2012: 161527.
 46. Mohd Ramli ES, Ahmad F, Salleh NI, et al. Beneficial effects of annatto (Bixa Orellana) tocotrienol on bone histomorphometry and expression of genes related to bone formation and resorption in osteoporosis induced by dexamethasone. *Int J Med Res Health Sci* 2018; 7: 85-100.
 47. Lee JY, Hong SH. Hematopoietic stem cells and their roles in tissue regeneration. *Int J Stem Cells* 2020; 13: 1-12.
 48. Brown MG, Brady DJ, Healy KM, Henry KA, Ogunsola AS, Ma X. Stem cells and acellular preparations in bone regeneration/fracture healing: current therapies and future directions. *Cells* 2024; 13: 1045.
 49. Sarkar SK, Lee BY, Padalhin AR, et al. Brushite-based calcium phosphate cement with multichannel hydroxyapatite granule loading for improved bone regeneration. *J Biomater Appl* 2016; 30: 823-37.
 50. Olszta MJ, Cheng X, Jee SS, et al. Bone structure and formation: a new perspective. *Materials Sci Engineering R Rep* 2007; 58: 77-116.
 51. Shahrin Z, Makpol S, Tan GC, Muhammad NA, Hasan ZAA. Topical application of the palm tocotrienol-rich fraction (TRF) enhances cutaneous wound healing in type 2 diabetic mice. *J Oil Palm Res* 2022; 34: 546-61.
 52. Schneider MR. Von Kossa and his staining technique. *Histochem Cell Biol* 2021; 156: 523-6.
 53. Ekeuku SO, Nor Muhamad ML, Aminuddin AA, et al. Effects of emulsified and non-emulsified palm tocotrienol on bone and joint health in ovariectomised rats with monosodium iodoacetate-induced osteoarthritis. *Biomed Pharmacother* 2024; 170: 115998.
 54. Zhang Y, Shen L, Mao Z, et al. Icariin enhances bone repair in rabbits with bone infection during post-infection treatment and prevents inhibition of osteoblasts by vancomycin. *Front Pharmacol* 2017; 8: 784.
 55. Chin KY, Abdul-Majeed S, Mohamed N, Ima-Nirwana S. The effects of tocotrienol and lovastatin co-supplementation on bone dynamic histomorphometry and bone morphogenetic protein-2 expression in rats with estrogen deficiency. *Nutrients* 2017; 9: 143.
 56. Wan Hasan WN, Chin KY, Abd Ghafar N, Soelaiman IN. Annatto-derived tocotrienol promotes mineralization of MC3T3-E1 cells by enhancing BMP-2 protein expression via inhibiting RhoA activation and HMG-CoA reductase gene expression. *Drug Des Devel Ther* 2020; 14: 969-76.
 57. Abukhadir SS, Mohamed N, Makpol S, Muhammad N. Effects of palm vitamin e on bone-formation-related gene expression in nicotine-treated rats. *Evid Based Complement Alternat Med* 2012; 2012: 656025.
 58. Mohamad NV, Soelaiman IN, Chin KY. Effects of tocotrienol from Bixa orellana (annatto) on bone histomorphometry in a male osteoporosis model induced by busferelin. *Biomed Pharmacother* 2018; 103: 453-62.
 59. Singh S, Kumar D, Lal AK. Serum osteocalcin as a diagnostic biomarker for primary osteoporosis in women. *J Clin Diagn Res* 2015; 9: Rc04-07.
 60. Tateiwa D, Nakagawa S, Tsukazaki H, et al. A novel BMP-2-loaded hydroxyapatite/beta-tricalcium phosphate microsphere/hydrogel composite for bone regeneration. *Sci Rep* 2021; 11: 16924.
 61. Jiang C, Zhu S, Zhan W, Lou L, Li A, Cai J. Comparative analysis of bone turnover markers in bone marrow and peripheral blood: implications for osteoporosis. *J Orthop Surg Res* 2024; 19: 163.
 62. Hogan HA, Ruhmann SP, Sampson HW. The mechanical properties of cancellous bone in the proximal tibia of ovariectomized rats. *J Bone Miner Res* 2000; 15: 284-92.
 63. Wong SK, Chin KY, Ima-Nirwana S. The effects of tocotrienol on bone peptides in a rat model of osteoporosis induced by metabolic syndrome: the possible communication between bone cells. *Int J Environ Res Public Health* 2019; 16: 3313.
 64. Wong SK, Kamisah Y, Mohamed N, et al. Potential role of tocotrienols on non-communicable diseases: a review of current evidence. *Nutrients* 2020; 12: 259.